



# The Pathway To Establishing HIV Latency Is Critical to How Latency Is Maintained and Reversed

Simin D. Rezaei,<sup>a,b</sup> Hao K. Lu,<sup>a\*</sup> J. Judy Chang,<sup>a</sup> Ajantha Rhodes,<sup>a</sup> Sharon R. Lewin,<sup>a,c</sup>  Paul U. Cameron<sup>a,c</sup>

<sup>a</sup>The Peter Doherty Institute for Infection and Immunity, The University of Melbourne and Royal Melbourne Hospital, Melbourne, Australia

<sup>b</sup>Department of Microbiology and Immunology, The University of Melbourne at the Peter Doherty Institute for Infection and Immunity, Melbourne, Australia

<sup>c</sup>Department of Infectious Diseases, Alfred Hospital and Monash University, Melbourne, Australia

**ABSTRACT** HIV infection requires lifelong antiretroviral therapy because of the persistence of latently infected CD4<sup>+</sup> T cells. The induction of virus expression from latently infected cells occurs following T cell receptor (TCR) activation, but not all latently infected cells respond to TCR stimulation. We compared two models of latently infected cells using an enhanced green fluorescent protein (EGFP) reporter virus to infect CCL19-treated resting CD4<sup>+</sup> (rCD4<sup>+</sup>) T cells (preactivation latency) or activated CD4<sup>+</sup> T cells that returned to a resting state (postactivation latency). We isolated latently infected cells by sorting for EGFP-negative (EGFP<sup>-</sup>) cells after infection. These cells were cultured with antivirals and stimulated with anti-CD3/anti-CD28, mitogens, and latency-reversing agents (LRAs) and cocultured with monocytes and anti-CD3. Spontaneous EGFP expression was more frequent in postactivation latency than in preactivation latency. Stimulation of latently infected cells with monocytes/anti-CD3 resulted in an increase in EGFP expression compared to that for unstimulated controls using the preactivation latency model but led to a reduction in EGFP expression in the postactivation latency model. The reduced EGFP expression was not associated with reductions in the levels of viral DNA or T cell proliferation but depended on direct contact between monocytes and T cells. Monocytes added to the postactivation latency model during the establishment of latency reduced spontaneous virus expression, suggesting that monocyte-T cell interactions at an early time point postinfection can maintain HIV latency. This direct comparison of pre- and postactivation latency suggests that effective strategies needed to reverse latency will depend on how latency is established.

**IMPORTANCE** One strategy being evaluated to eliminate latently infected cells that persist in HIV-infected individuals on antiretroviral therapy (ART) is to activate HIV expression or production with the goal of inducing virus-mediated cytolysis or immune-mediated clearance of infected cells. The gold standard for the activation of latent virus is T cell receptor stimulation with anti-CD3/anti-CD28. However, this stimulus activates only a small proportion of latently infected cells. We show clear differences in the responses of latently infected cells to activating stimuli based on how latent infection is established, an observation that may potentially explain the persistence of noninduced intact proviruses in HIV-infected individuals on ART.

**KEYWORDS** T cells, human immunodeficiency virus, latency, monocytes

Antiretroviral (ARV) therapy (ART) has dramatically reduced morbidity and mortality, but treatment is lifelong, and there is no cure. This is because HIV can persist in long-lived and proliferating latently infected CD4<sup>+</sup> T cells (1, 2). Latency is established within days following infection (3) and can be established in multiple different T cell

Received 2 January 2018 Accepted 8 April 2018

Accepted manuscript posted online 11 April 2018

**Citation** Rezaei SD, Lu HK, Chang JJ, Rhodes A, Lewin SR, Cameron PU. 2018. The pathway to establishing HIV latency is critical to how latency is maintained and reversed. *J Virol* 92:e02225-17. <https://doi.org/10.1128/JVI.02225-17>.

**Editor** Guido Silvestri, Emory University

**Copyright** © 2018 American Society for Microbiology. All Rights Reserved.

Address correspondence to Paul U. Cameron, paul.cameron@unimelb.edu.au.

\* Present address: Hao K. Lu, Agency for Science, Technology and Research, Singapore.

subsets (4–6). It is now clear that latently infected cells are a heterogeneous population of CD4<sup>+</sup> T cells with different life spans (4), proliferative capacities (4, 7, 8), and frequencies of intact or defective virus (9, 10). Therefore, eliminating latency through activation or permanent silencing remains a major challenge.

HIV latency can be established through multiple pathways. Broadly, these pathways may be defined as preactivation latency, involving the direct infection of resting CD4<sup>+</sup> (rCD4<sup>+</sup>) T cells (11–13), and postactivation latency, involving either infection of activated cells and reversion to a resting state or direct infection of T cells transitioning from effector memory to resting central memory cells after T cell receptor (TCR) stimulation (14–16).

One approach to eliminate or reduce latent infection is to activate HIV production from latently infected cells to induce virus-mediated cytolysis or immune-mediated clearance of infected cells. Activation of T cells with anti-CD3/anti-CD28 or a mitogen, such as phytohemagglutinin (PHA), phorbol 12-myristate 13-acetate (PMA), or ionomycin (8, 17), induces virus expression; however, it is now clear that some latently infected cells do not respond to a single stimulus but require multiple repeated stimulations (18). These viruses have no major sequence defects and are now referred to as intact noninduced proviruses (9, 17, 19). In addition, the frequencies of virus production from the same stimulus differ across *in vitro*-derived latently infected cells (20–22) and *ex vivo* stimulation of CD4<sup>+</sup> T cells from HIV-infected individuals on ART (17, 19). These observations suggested to us that the activation of virus production from latency is not completely linked to TCR stimulation and that alternative signaling pathways may be required to reverse latency.

There are multiple paths to HIV expression in activated T cells, which include the activation of protein kinase C (PKC), calcineurin, nuclear factor of activated T cells (NFAT) and nuclear factor kappa light chain activator of B cells (NF- $\kappa$ B) signaling pathways, epigenetic modifiers, and transcriptional regulators (14, 23, 24). Direct contact between immature monocyte-derived dendritic cells (DCs) (iMDDCs) and latently infected cells has been shown to induce virus expression in activated T cells *in vitro* (25). In a similar study screening a group of antigen-presenting cells (APCs), blood-derived myeloid DCs (i.e., CD1c<sup>+</sup> and CD141<sup>+</sup>), gut-associated DCs (CD103<sup>+</sup>), and mature myeloid DCs were able to induce virus expression in effector T cells (26).

T cell interactions with antigen-presenting cells initiate TCR signaling (signal 1), additional costimulatory signaling (signal 2), as well as cytokine signaling (signal 3). The contributions of costimulation and soluble factors will differ according to the antigen-presenting cell and the specific T cell subset in the cocultures. Anti-CD3/anti-CD28 provides both TCR signaling and CD28 costimulation, but monocytes and anti-CD3 can provide similar TCR signaling and CD28 costimulation as well as monocyte-derived costimulation and soluble factors. Although previous work suggested that T cell activation pathways initiated by APCs can induce virus expression in latently infected activated T cells (25, 26), those studies did not determine the effect of APCs on virus expression from latency established by defined pathways.

In this study, we compared latency reversal in pre- and postactivation models of latency. We used primary T cells, which differed in activation status at the time of infection. Using monocytes as APCs, we showed that coculturing latently infected primary T cells with monocytes and soluble anti-CD3 resulted in a significant increase in virus expression compared to the spontaneous expression in a preactivation latency model. Virus expression was significantly greater than that with stimulation with anti-CD3/anti-CD28. In contrast, in a model of postactivation latency, monocyte/anti-CD3 stimulation significantly reduced virus expression from latently infected cells compared to spontaneous expression. To further investigate the effect of the establishment of the latency on latency reversal, we also tested mitogens and a panel of latency-reversing agents (LRAs). Our data show that latently infected cells generated via preactivation and postactivation pathways have different responses to the same stimulation. Furthermore, monocytes actively maintained latency in a postactivation latency

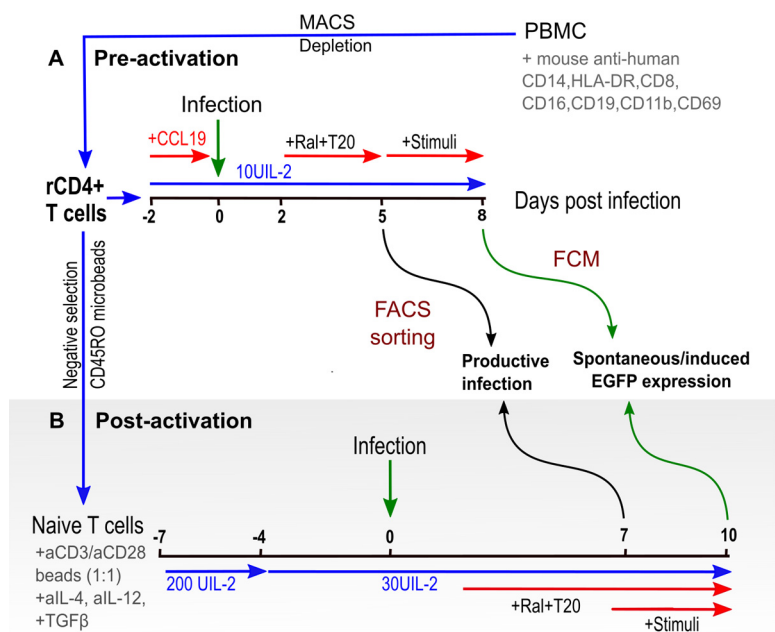


**FIG 1** Establishment of pre- and postactivation latency in primary T cells *in vitro*. (A) Preactivation latency. Resting CD4<sup>+</sup> T cells were isolated from PBMCs of healthy blood donors by negative selection using MACS, pretreated with CCL19 (100 nM) for 24 h, and infected with NL4.3-EGFP at an MOI of 0.5. Further rounds of infection were blocked by the addition of antiretrovirals at 2 days postinfection and maintained during culture. Cells expressing EGFP (EGFP<sup>+</sup>) were enumerated and removed by FCM sorting at day 5 postinfection. EGFP<sup>-</sup> cells was determined by FCM after activation in the presence of the antiretroviral. (B) Postactivation latency. Naive T cells were sorted from total CD4<sup>+</sup> T cells by negative selection using CD45RO microbeads. Cells were activated with anti-CD3/anti-CD28 beads with anti-IL-4, anti-IL-12, and TGF-β. Beads were removed at day 3, and cells were expanded in 30 U IL-2 for 4 days. At day 7 postactivation, cells were infected with NL4.3-EGFP. Antiretrovirals were added to the cultures at 2 days postinfection and maintained during culture. At day 7 postinfection, EGFP-expressing cells were enumerated and removed by FCM sorting, and EGFP<sup>-</sup> cells were activated with the same panel of stimuli used in the preactivation model. EGFP expression was measured at 3 days poststimulation by FCM. Ral, raltegravir; FACS, fluorescence-activated cell sorter.

model. We conclude that effective strategies needed to reverse latency will depend on how latency is established.

**RESULTS**

**Generation of latently infected primary T cells.** The two different primary cell models of latency were generated by using CD4<sup>+</sup> T cells isolated from the same donors to establish preactivation latency (11) and postactivation latency (14). T cells from both models were infected with replication-competent HIV-1<sub>NL4.3</sub> with an enhanced green fluorescent protein (EGFP) reporter (Fig. 1). In both models, EGFP-negative (EGFP<sup>-</sup>) cells were sorted by flow cytometry (FCM) (Fig. 1), and the effects of different activation stimuli were determined and compared to those in unstimulated cells cultured in media and with ARVs alone.

The expression of EGFP was detected in the preactivation latency model at day 3 and in the postactivation model at day 1 (see Fig. S1A in the supplemental material). Productive infection was detected as EGFP expression at day 5 in preactivation latency and at day 7 in postactivation latency. The level of productive infection was significantly lower in the preactivation model than in the postactivation model (Fig. 2A). Sorting by flow cytometry was used to remove EGFP-expressing cells (Fig. S1B). Without the removal of productively infected cells, the expression of EGFP could not be reliably detected in the cultures (Fig. S1C). Postsort expression of EGFP was undetectable in most cultures; thus, the expression of EGFP after stimulation was used as a measure of inducible latent infection. Following the isolation of EGFP<sup>-</sup> cells, the level of spontaneous EGFP expression in unstimulated cultures was higher in postactivation than in preactivation latency.

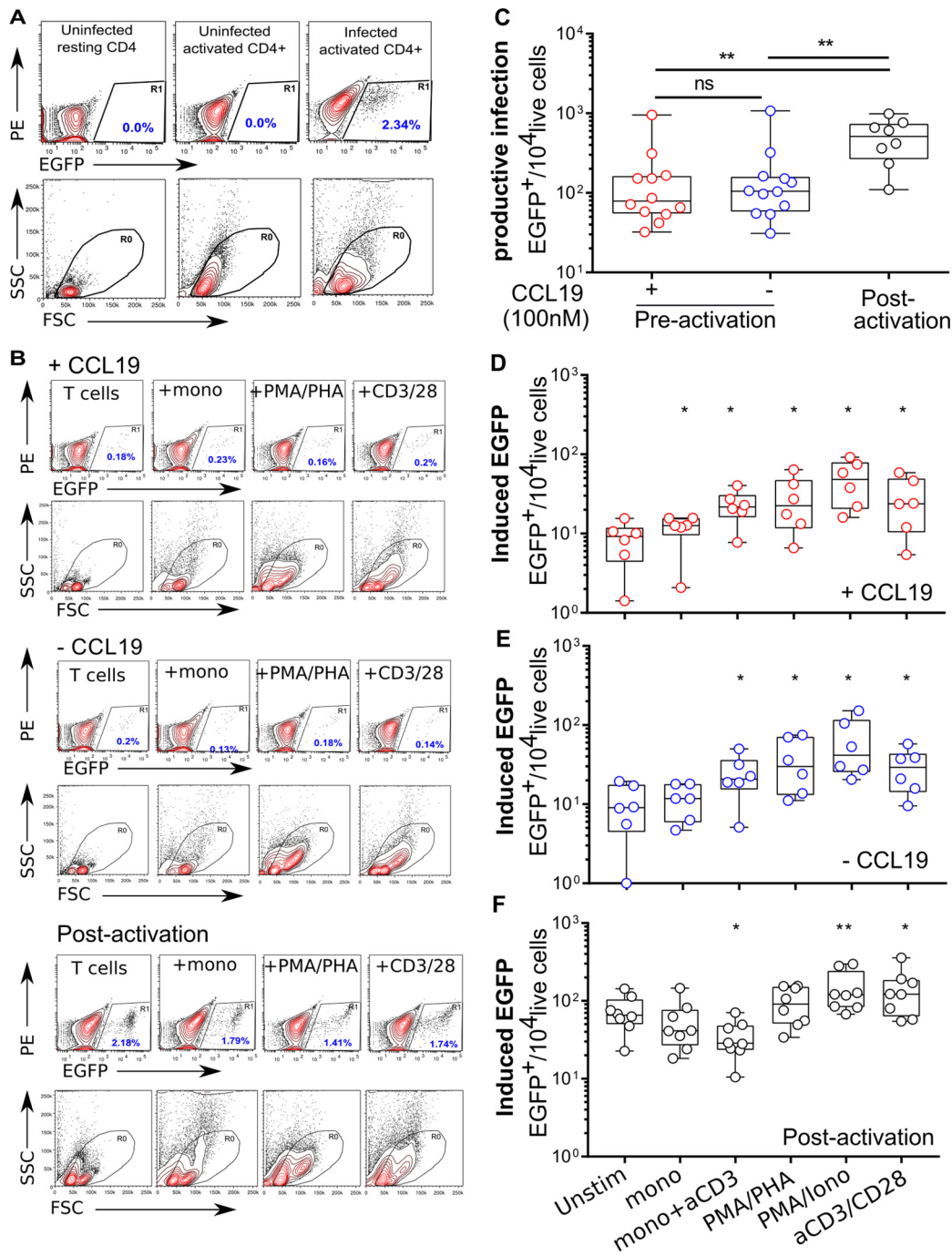


**FIG 2** HIV infection and virus reactivation in pre- and postactivation latency. (A) Flow cytometry gating and analysis used to measure EGFP expression in CD4<sup>+</sup> T cells using the *in vitro* latency models. Live cells were defined by forward scatter (FSC) versus side scatter (SSC). Uninfected T cells were used to detect any background EGFP expression in our system. EGFP expression was measured against the PE channel. Plots show EGFP expression in mock-infected T cells (uninfected resting CD4<sup>+</sup>) with chemokine treatment (+CCL19) or mock-activated T cells (uninfected activated CD4<sup>+</sup>) and infected T cells (activated CD4<sup>+</sup>). (B) Plots representing EGFP expression following activation. Data are shown as percentages of EGFP in each plot in preactivation (+CCL19 or untreated CD4<sup>+</sup> T cells) or postactivation latency. Data are representative of results for a matched sample in one experiment. (C) Frequency of productive infection in infected CD4<sup>+</sup> T cells measured by EGFP expression at 5 days postinfection in the preactivation models (CCL19 treated [+]) [red open circles] and untreated [-] [blue open circles] and at day 7 in the postactivation model (black open circles). (D to F) Induced EGFP expression was measured following stimulation of sorted EGFP<sup>-</sup> cells in preactivation latency with CCL19 (D) or without CCL19 (E) and in postactivation latency (F), using monocytes (mono), monocytes and anti-CD3 (20 μg/ml) (mono+aCD3), PHA (10 μg/ml) and PMA (50 ng/ml) (PMA/PHA), or PMA and ionomycin (500 ng/ml) (PMA/Iono) as well as plate-bound anti-CD3 (20 μg/ml) and anti-CD28 (3.6 μg/ml) (aCD3/aCD28) stimulation or culturing with antiretrovirals only (Unstim). EGFP expression was measured 72 h after coculture. Each dot represents data for a single donor, and the box plots show 25th and 75th percentiles, medians, and ranges. \*,  $P \leq 0.05$ ; \*\*,  $P \leq 0.01$  (as determined by a Wilcoxon matched-pairs signed-rank test).

In preactivation latency, the frequency of EGFP expression in response to the activation stimuli was significantly higher than that of spontaneous EGFP expression (Fig. 2B and C). The levels of infection and the frequency of EGFP expression in response to anti-CD3/anti-CD28 and the mitogens PMA-PHA and PMA-ionomycin compared to unstimulated controls were similar in both CCL19-treated and untreated cultures. Despite similar levels of infection in both T cell cultures, stimulation with monocytes led to a significantly greater increase in EGFP expression in CCL19-treated cultures than in cultures without CCL19 (Fig. 2B and C).

In postactivation latency, EGFP expression was significantly increased following stimulation with anti-CD3/anti-CD28 and PMA-ionomycin (Fig. 2D). The frequency of EGFP expression following coculture with monocytes or stimulation with PMA-PHA was similar to that of spontaneous EGFP expression. In contrast, EGFP expression was reduced after stimulation with monocytes/anti-CD3 compared to the unstimulated cultures (Fig. 2D).

To assess whether sorting induces virus expression independent of reactivation, in both latency models, we cocultured EGFP<sup>-</sup> cells with and without sorting and measured EGFP expression with and without stimulation with anti-CD3/anti-CD28 (Fig. S1). Sorting did not change the levels of EGFP expression or the viability of EGFP<sup>-</sup> cells in the culture system in the pre- and postactivation latency models.

In summary, we showed that coculture with monocytes/anti-CD3 induced viral EGFP expression in preactivation latency. However, this stimulation reduced EGFP expression in postactivation latency.

**Monocyte/anti-CD3 stimulation of EGFP expression in preactivation latency.** To understand how monocytes might reduce EGFP expression in postactivation latency but not in preactivation latency, we compared the effects of irradiated and nonirradiated monocytes with and without anti-CD3 on EGFP expression. In preactivation latency, there was no statistically significant difference in the frequencies of EGFP expression using irradiated or nonirradiated monocytes (Fig. 3A and B). In contrast, in postactivation latency, the use of irradiated monocytes significantly increased the frequency of EGFP expression with or without anti-CD3 (Fig. 3C). These data suggested that the inhibitory effect of monocytes in postactivation latency was radiation sensitive.

Since TCR activation in response to anti-CD3 requires cross-linking on the culture plate or by binding to the Fc receptor expressed on monocytes (27), we next determined whether the effect of monocytes in our system was due to differences in the efficiencies of cross-linking of CD3. Sorted EGFP<sup>-</sup> cells from the postactivation latency model were cocultured with monocytes in combination with soluble anti-CD3 or with anti-CD3/anti-CD28 beads (at 1:1 ratios with T cells). We found significantly reduced EGFP expression from infected T cells if they were cocultured with monocytes with either anti-CD3 or anti-CD3/anti-CD28 beads (Fig. 3D). Neither anti-CD3 alone nor anti-CD3/anti-CD28 beads with monocytes were statistically different from unstimulated cells from postactivation latency. These data suggest that the addition of monocytes actively inhibited EGFP expression in cultures in the presence of an activating signal from anti-CD3 and anti-CD3/anti-CD28 beads.

**Monocyte/anti-CD3 induces proliferation in pre- and postactivation latency.** To determine if the inhibition of EGFP expression by monocytes in postactivation latency was a result of reduced activation and proliferation, sorted EGFP<sup>-</sup> cells were labeled with eFluor670, and dye dilution was measured after 3 days of stimulation. Monocytes were excluded from the FCM analysis using the surface marker CD14 (see Fig. S2 in the supplemental material). In both models, T cell proliferation was significantly increased in pre- and postactivation latency following stimulation, with similar rankings of proliferation across the different activation stimuli (Fig. 4A). The levels of T cell proliferation in response to the addition of monocytes alone, PMA-ionomycin, anti-CD3/anti-CD28, PMA-PHA, and monocytes-anti-CD3 were significantly higher than those in unstimulated cultures, as expected (Fig. 4A).

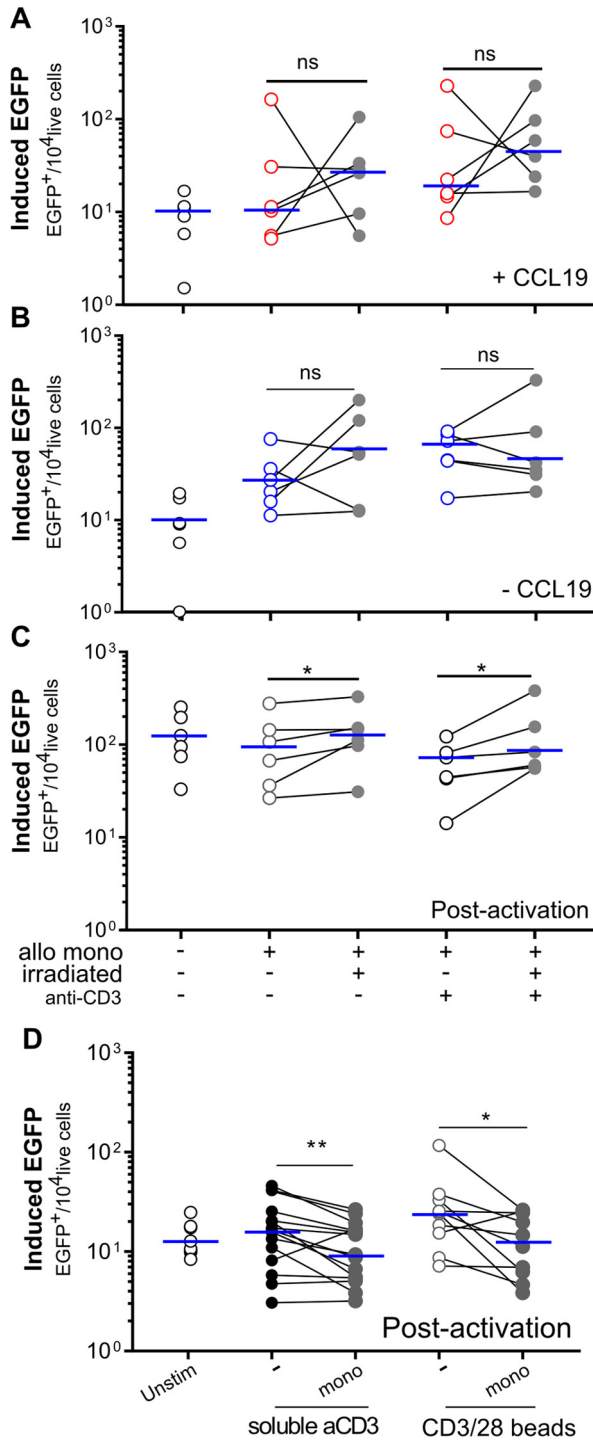


**FIG 3** EGFP expression following the addition of irradiated allogeneic monocytes. EGFP<sup>-</sup> cells were sorted and cocultured with allogeneic monocytes with or without soluble anti-CD3 (+, anti-CD3 [20 μg/ml]) in the presence of antiretrovirals. Monocytes were irradiated (+irr) (closed symbols) or nonirradiated (-irr) (open symbols) and added to latently infected EGFP<sup>-</sup> T cells. EGFP expression was measured at 72 h. (A to C) CCL19-treated (A) or untreated (B) cells and cells during postactivation latency (C). Each symbol represents data for a single donor. \*,  $P \leq 0.05$ ; ns, not significant (as determined by a Wilcoxon matched-pairs signed-rank test). Blue lines indicate the median. (D) Comparison of the frequencies of induced EGFP expression following stimulation with soluble anti-CD3 with or without monocytes and anti-CD3/anti-CD28 beads (with or without monocytes) in the postactivation model. Sorted EGFP<sup>-</sup> cells were cocultured with soluble anti-CD3 (20 μg/ml) or with anti-CD3/anti-CD28 beads (1:1 ratio) with and without monocytes in the presence of antiretrovirals. Induced EGFP expression was measured at 72 h. Each point represents data for a single donor. \*,  $P \leq 0.05$ ; \*\*,  $P \leq 0.01$  (as determined by a Wilcoxon matched-pairs signed-rank test). The median is indicated with a blue line.

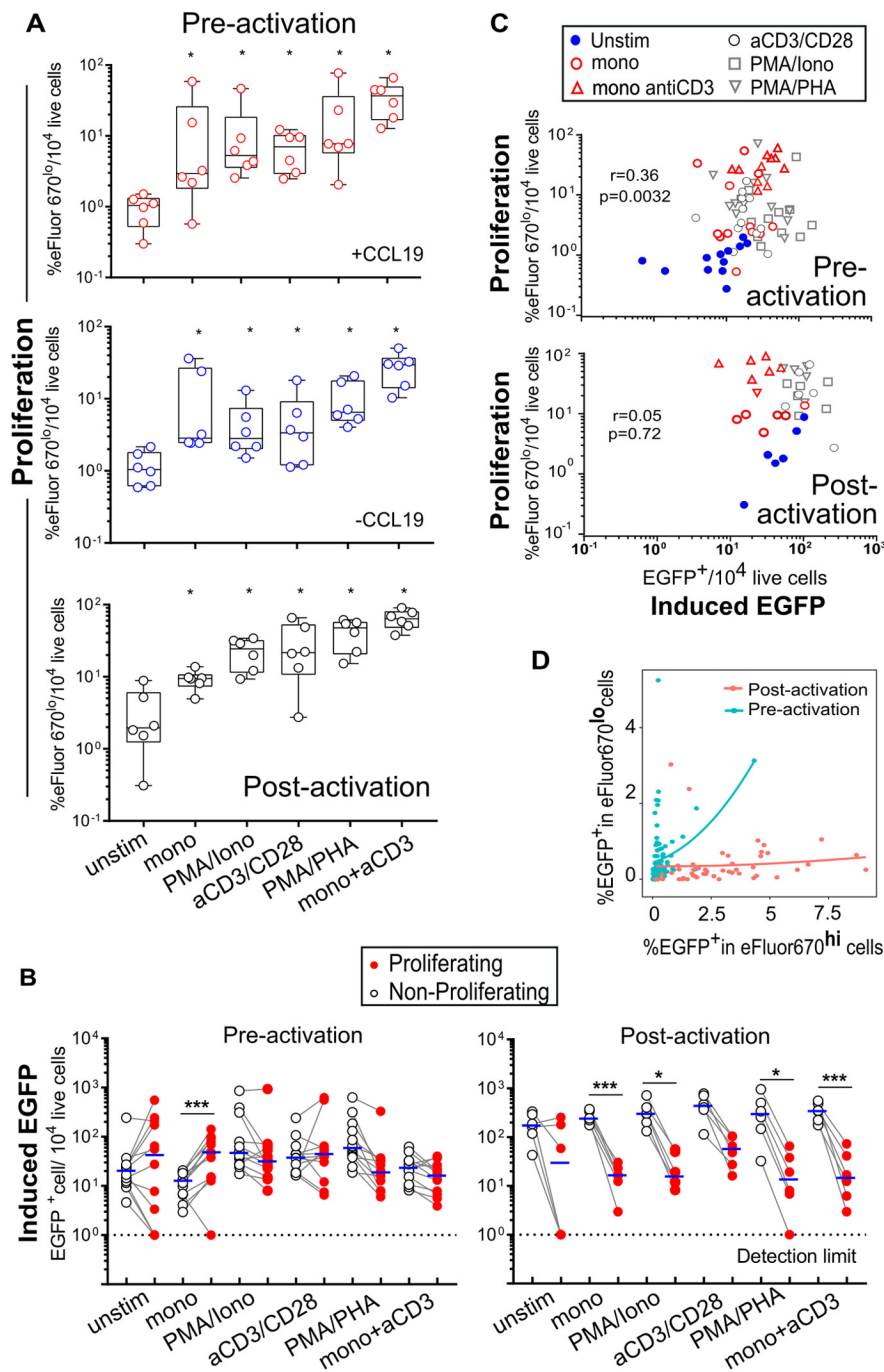


**FIG 4** Cellular proliferation and virus expression from sorted EGFP<sup>-</sup> cells following stimulation. (A) Levels of cell proliferation following treatment with different stimuli. The sorted EGFP<sup>-</sup> T cells in the preactivation models (CCL19 treated [+] [open red circles] and untreated [-] [open blue circles]) and postactivation models were stained with proliferation dye (eFluor670) and then cocultured with allogeneic monocytes, with and without anti-CD3, plate-bound anti-CD/anti-CD28, or PMA-PHA and PMA-ionomycin, or with an antiretroviral alone (unstim). At 72 h postactivation, cellular proliferation was measured by FCM. Each point represents data for an individual donor; the box plots show 25th and 75th percentiles, medians, and ranges. \*,  $P \leq 0.05$  (as determined by a Wilcoxon matched-pairs signed-rank test). (B) EGFP expression in nonproliferating (eFluor670<sup>hi</sup>) and proliferating (eFluor670<sup>lo</sup>) cells under each stimulation condition. Each point represents data for a single donor. \*,  $P \leq 0.05$ ; \*\*\*,  $P \leq 0.001$  (as determined by a Wilcoxon matched-pairs signed-rank test). The median is shown as a blue line. (C) Correlation between EGFP expression and cell proliferation in pre- and postactivation latency, determined by using Spearman's rank test. (D) Correlation between the frequency of EGFP expression in nonproliferating (eFluor670<sup>hi</sup>) and proliferating (eFluor670<sup>lo</sup>) cells in both models. Data from all cultures were pooled, and the level of EGFP expression in nonproliferating (eFluor670<sup>hi</sup>) cells was plotted against the level of EGFP expression in proliferating (eFluor670<sup>lo</sup>) cells in both models.

We then examined EGFP expression in both proliferating (eFluor670<sup>lo</sup>) and nonproliferating (eFluor670<sup>hi</sup>) latently infected cells in the two models (Fig. 4B). In the preactivation model, differences between the frequencies of EGFP expression from nonproliferating (eFluor670<sup>hi</sup>) and proliferating (eFluor670<sup>lo</sup>) cells did not reach statistical significance, except when monocytes were present in the cocultures (Fig. 4B).

In postactivation latency, we found more-frequent EGFP expression in nonproliferating (eFluor670<sup>hi</sup>) cells than in proliferating (eFluor670<sup>lo</sup>) cells, and these differences were significant following stimulation with monocytes, PMA-ionomycin, PMA-PHA, and monocyte-anti-CD3 cocultures (Fig. 4B). The level of EGFP expression from nonproliferating (eFluor670<sup>hi</sup>) cells was significantly higher in the postactivation latency model than in matched cultures in the preactivation latency model (Fig. S3A and S3B).

We determined the correlation between T cell proliferation and EGFP expression after stimulation in the two latency models. There was a significant correlation between T cell proliferation and EGFP expression in the preactivation model but not in the postactivation latency model, where the high frequency of EGFP expression was independent of the level of proliferation (Fig. 4C). In the postactivation model, coculture with monocytes (with and without anti-CD3) led to a population of cells with high levels of cellular proliferation and low frequencies of EGFP expression (Fig. 4C).

We then compared the EGFP expression levels of proliferating and nonproliferating cells in both models (Fig. 4D). In preactivation latency, there was a higher frequency of EGFP expression in proliferating than in nonproliferating T cells (Fig. 4D). In contrast, there was a high frequency of EGFP expression in nonproliferating compared to proliferating cells in the postactivation model (Fig. 4D). A similar pattern was observed for the distributions of EGFP-expressing cells in proliferating (eFluor670<sup>lo</sup>) and nonproliferating (eFluor670<sup>hi</sup>) T cells relative to the levels of T cell proliferation (eFluor670<sup>lo</sup>) (Fig. S3C). The observed increase in EGFP expression levels in nonproliferating cells and the decreased expression levels in proliferating cells in postactivation latency could be attributed to a preferential expansion of noninfected cells and progressive enrichment for EGFP expression in nonproliferating cells (Fig. S3C).

Since CCL19 is the homeostatic ligand of CCR7 (28) and can inhibit T cell proliferation (29), we compared the distributions of EGFP-expressing cells in nonproliferating (eFluor670<sup>hi</sup>) and proliferating (eFluor670<sup>lo</sup>) CCL19-treated CD4<sup>+</sup> T cells. There was no statistically significant difference in the frequency of nonproliferating (eFluor670<sup>hi</sup>) cells treated with CCL19 (Fig. S4). However, there was a significant reduction in the frequency of EGFP-expressing cells among proliferating cells in the presence of CCL19 treatment (Fig. S4). This finding supports our previous work whereby the treatment of CD4<sup>+</sup> T cells with CCL19 can lead to increased latent infection and a reduction in spontaneous virus expression (21, 30); thus, subsequent preactivation latency was established in the presence of CCL19.

#### **Spontaneous expression from latency correlates with productive infection.**

Low-level transcription from latently infected T cells, as measured by cell-associated unspliced HIV RNA, has been described for HIV-infected individuals on suppressive ART (31–33). In addition, *in vitro*, the spontaneous expression of either EGFP or Gag without exogenous stimulation has been demonstrated (34, 35). We found a significantly lower frequency of spontaneous EGFP expression in the preactivation latency than in the postactivation latency model with matched donors (Fig. 5A).

We examined the relationship between the frequency of spontaneous EGFP expression and the frequency of productively infected cells (productive infection) prior to the isolation of the EGFP<sup>+</sup> cells in both *in vitro* latency models (Fig. 5B). There was no significant correlation within the models, but when the two models were combined, we found a significant correlation between productive infection and the spontaneous expression of EGFP (Fig. 5B). We found no relationship between postsort and spontaneous EGFP expression levels (Fig. 5C) or between productive and postsort EGFP expression levels (Fig. 5D). These data are potentially consistent with spontaneous EGFP expression representing cells that are on their way to productive infection. However, given that we used ARVs early after infection to block further rounds of infection, the



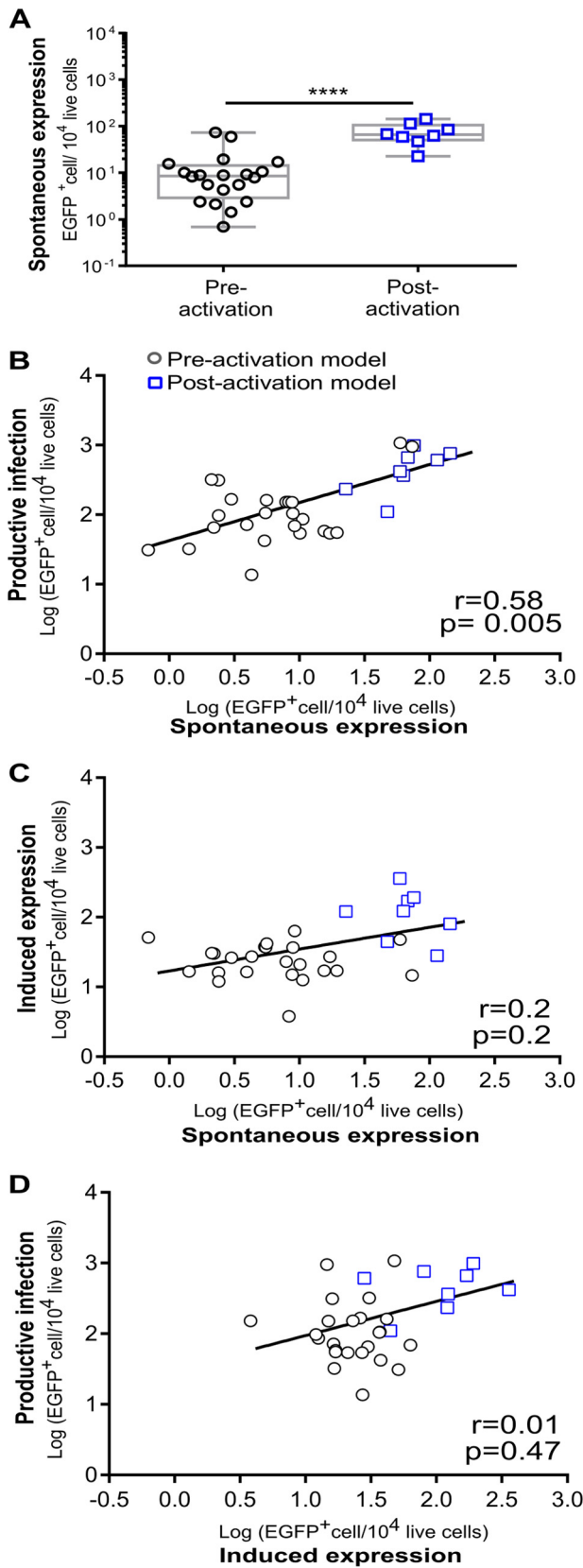


**FIG 5** Postsort spontaneous EGFP expression is associated with higher-level productive infection. (A) The level of spontaneous EGFP expression from infected cells was measured 72 h after coculture of sorted EGFP<sup>-</sup> cells with antiretrovirals only. Each point represents data for an individual donor; the box plots show 25th and 75th percentiles, medians, and ranges. \*\*\*\*,  $P \leq 0.0001$  (as determined by a Mann-

(Continued on next page)

direct relationship between productive and subsequent spontaneous EGFP expression may represent a continuing stochastic process of EGFP expression from latency.

**Responses to latency reversal in pre- and postactivation latency.** We determined whether the reversal of latent infection with commonly used LRAs also differed in pre- and postactivation latency. Latently infected cells in both *in vitro* models were stimulated with a panel of LRAs, including the histone deacetylase (HDAC) inhibitors panobinostat (Pan) and romidepsin (Rom), the bromodomain and extra-terminal motif (BET) bromodomain inhibitor JQ1, the  $\gamma$ c chain cytokine interleukin-7 (IL-7), the PKC agonist bryostatin-1 (Bryo-1), and the nonspecific histone lysine methyltransferase enzyme chaetocin (CTN) (see Fig. S5 in the supplemental material). In preactivation latency, EGFP expression was detected after stimulation with romidepsin and anti-CD3/anti-CD28, as expected. The level of EGFP expression was significantly above the background level detected in dimethyl sulfoxide (DMSO)-treated cultures (Fig. S5). Stimulation with bryostatin-1, JQ1, and panobinostat induced a 3-fold increase in EGFP expression levels compared to those with DMSO treatment, while IL-7- and CTN-treated cultures induced minimal increases in EGFP expression levels above the background level (Fig. S5).

In postactivation latency, there was no significant increase in EGFP expression after stimulation with bryostatin-1, romidepsin, and anti-CD3/anti-CD28 compared to background expression levels with DMSO (Fig. S5). The matched samples in the pre- and postactivation latency models showed significantly different responses to LRAs. There was a significant response to the HDACs panobinostat and romidepsin and to JQ1 in the preactivation model compared to the postactivation model (Fig. S5C). These data suggest that latency may be less critically dependent on epigenetic control in postactivation latency than in preactivation latency. Alternatively, these drugs may have different rates of uptake or pharmacodynamics in these two models.

**Activation increases the proportion of latently infected cells expressing EGFP in preactivation latency.** Possible explanations for the low frequency of EGFP expression in proliferating cells in postactivation latency and the apparent decrease in EGFP expression after monocyte/anti-CD3 stimulation are (i) active suppression of virus expression during the proliferation of T cells responding to stimulation, (ii) preferential expansion of uninfected T cells to give an apparent decrease in EGFP expression simply through dilution during the expansion of predominantly uninfected T cells, or (iii) preferential cell death in uninfected nonproliferating cells. To address this question, we compared EGFP expression to the frequency of HIV DNA in these cultures. We expected a higher frequency of latency measured by HIV DNA than by EGFP expression in cultures. Second, we expected that the frequency of HIV DNA would decline or remain unchanged following T cell proliferation in the presence of ARVs if latently infected cells proliferated and productive infection was associated with reduced cell survival.

In the preactivation latency model, a significant reduction in the frequency of HIV DNA was observed after stimulation with monocytes–anti-CD3 and anti-CD3/anti-CD28, which coincided with an increase in the frequency of EGFP expression (Fig. 6A and B). By expressing the frequency of EGFP-positive (EGFP<sup>+</sup>) cells as a fraction of HIV DNA (EGFP/DNA), we showed that 24.6%, 54.6%, and 94.3% of the total infected cells expressed EGFP upon stimulation with monocytes–anti-CD3, PMA-ionomycin, and anti-CD3/anti-CD28, respectively (Fig. 6C).

In postactivation latency, there was no significant change in the proportions of EGFP-expressing cells in T cells following activation, and in keeping with the above-

#### FIG 5 Legend (Continued)

Whitney test). (B) Correlation between EGFP<sup>+</sup> productively infected T cells and EGFP expression from sorted EGFP<sup>-</sup> cells (spontaneous expression) 72 h after stimulation with monocytes, monocytes–anti-CD3 (20  $\mu$ g/ml), PHA (10  $\mu$ g/ml)–PMA (50 ng/ml), PMA–ionomycin (500 ng/ml), plate-coated anti-CD3 (20  $\mu$ g/ml)/anti-CD28 (3.6  $\mu$ g/ml), or antiretrovirals only. (C) Comparison of induced EGFP expression after stimulation and spontaneous expression (unstimulated expression). (D) Correlation between EGFP<sup>+</sup> productively infected cells and induced EGFP expression. Each point represents data for a single donor; correlations were determined by Spearman's rank test.

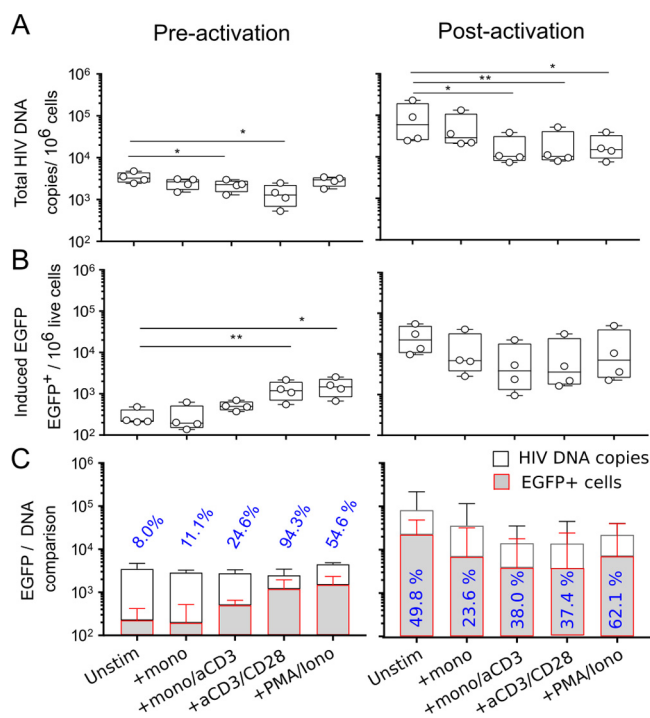


**FIG 6** Stimulation increases EGFP expression from T cells containing HIV DNA in preactivation latency. Sorted EGFP<sup>-</sup> cells from pre- and postactivation latency were cocultured with and without stimuli in the presence of antiretrovirals. (A) Total HIV DNA was measured 72 h after stimulation by using real-time PCR targeting *gag* 5' long terminal repeat (LTR) primers. (B) The number of EGFP-expressing cells was measured by FCM. Each dot represents data for an individual donor, and the box plots show 25th and 75th percentiles, medians, and ranges. \*,  $P \leq 0.05$ ; \*\*,  $P \leq 0.01$  (as determined by paired Student's *t* test). (C) Overlay bar graphs showing the number of EGFP-expressing cells compared to total HIV DNA/latent infection. The proportion (percentage) is indicated by the numerical ratio of EGFP-expressing cells per total latent infection. Bar graphs show medians and interquartile ranges.

described observations of high levels of spontaneous expression, a high proportion of EGFP expression compared to HIV DNA was detected in unstimulated cultures, i.e., 49.8% compared to 37.4% in anti-CD3/anti-CD28-treated cultures and 62.2% in PMA-ionomycin-treated cultures. The lowest proportions of EGFP expression compared to HIV DNA were observed in monocytes with and without anti-CD3 (23.6% and 38%, respectively) (Fig. 6C).

These data suggest that in the postactivation model, the reduction in the levels of EGFP expression following stimulation might be due to the active suppression of virus expression. However, our analysis does not take into account the distribution of latently infected cells between proliferating and nonproliferating T cells. The high levels of proliferation, the high levels of HIV expression in nonproliferating T cells, and the low levels of HIV expression in proliferating T cells may be explained by a partitioning of infected cells into the nonproliferating population and a loss of infected cells from proliferating cells through either cell death or the preferential expansion of uninfected cells.

**Suppression of virus expression by APCs during establishment of latency.** Since monocytes seem to prevent latency reversal in postactivation latency (Fig. 2C and 3), we next determined if direct contact between monocytes and T cells during the establishment of latency would reduce the high frequency of spontaneous expression in postactivation latency. Syngeneic monocytes were added directly or via transwells to cultures of infected T cells at day 2 postinfection. The EGFP expression level was compared to those in cocultures where latency was established in the absence of monocytes (T cells alone and PMA-ionomycin-activated T cells) (Fig. 7A). We did not find any significant differences in the frequencies of productive infection with and

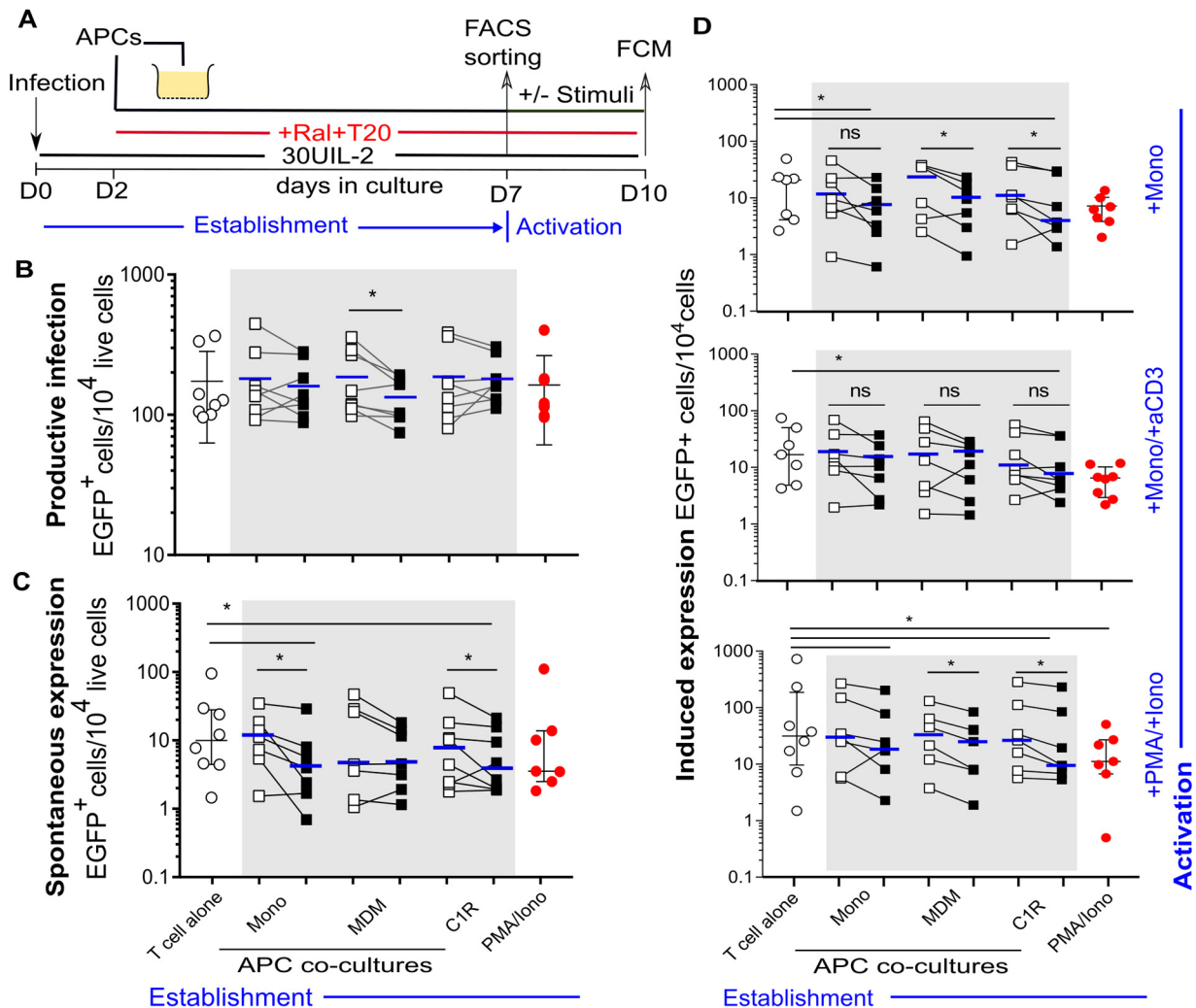


**FIG 7** Coculturing of APCs with activated infected T cells during establishment of latency inhibits subsequent inducible EGFP expression. (A) Infected T cells in postactivation latency were cocultured with APCs directly or in the bottom reservoir of a transwell system from day 2 postinfection. Antiretrovirals were added at the same time, and cells were cultured for 5 days. At day 7 postinfection, the EGFP<sup>-</sup> cells were sorted and cultured with or without stimulation. EGFP expression was measured by FCM. (B) Numbers of productively infected EGFP-expressing cells from APC-treated cultures with transwells (open squares) or without transwells (closed squares) and activation-induced expression compared to the number of productively expressing cells among T cells alone (open circles) and PMA-ionomycin-treated T cells (closed circles). The median is shown as a blue line. \*,  $P \leq 0.05$  (as determined by a Wilcoxon matched-pairs signed-rank test). Each dot represents data for an individual donor. APC cocultures during establishment of latency are shown by gray shading. (C) Numbers of spontaneous EGFP-expressing cells from T cells alone, APC cocultures, and mitogen-activated T cell cultures. The median is shown as a blue line. \*,  $P \leq 0.05$  (as determined by a Wilcoxon matched-pairs signed-rank test). APC cocultures during establishment of latency are shown by gray shading. (D) Numbers of induced EGFP-expressing cells following stimulation with monocytes, monocytes and anti-CD3 (20  $\mu\text{g/ml}$ ), and PMA (50 ng/ml)–ionomycin (500 ng/ml) compared to the level of EGFP expression following the same stimulation in cultures with CD4<sup>+</sup> T cells alone or mitogen-treated T cells. Each point represents data for a single donor. The median is shown as a blue line. \*,  $P \leq 0.05$  (as determined by a Wilcoxon matched-pairs signed-rank test). APC cocultures during the establishment of latency are shown by gray shading.

without monocytes, except when monocyte-derived macrophages (MDMs) were used as APCs (Fig. 7B). Spontaneous EGFP expression was reduced in T cells cocultured directly with monocytes during the establishment of latency, but this effect was not observed in the presence of a transwell (Fig. 7C). The frequency of spontaneous EGFP expression in T cell-monocyte cocultures was significantly lower than that in T cells cultured alone (Fig. 7C).

To determine if the reduction of spontaneous EGFP expression was monocyte specific, we also measured the frequency of spontaneous EGFP expression from cultures where syngeneic MDMs and irradiated Epstein-Barr virus (EBV)-transformed B cells (C1R) were used as APCs. Like monocytes, coculture with C1R cells significantly reduced

spontaneous expression from unstimulated cultures compared to that in cultures without APCs (Fig. 7C). We did not find a significant difference in the levels of spontaneous expression of EGFP when we used MDMs as APCs. These data suggest that both monocytes and C1R cells reduce spontaneous HIV expression from latently infected cells during direct contact.

We then looked at virus expression following the stimulation of latently infected cells generated during APC-T cell coculture (Fig. 7D). The direct interaction of infected T cells with both MDMs and C1R cells significantly reduced the induction of EGFP expression from latently infected cells in response to monocytes and mitogens compared to matched cultures when the interaction was blocked by using a transwell (Fig. 7D). Interestingly, we did not find a significant difference in induced EGFP expression from latently infected cells cocultured with syngeneic monocytes during the establishment of latency (Fig. 7D). These data showed that while the direct interaction between T cells and monocytes reduced spontaneous expression from latently infected cells, this interaction had no effect on virus expression in response to activation signals.

Taken together, these data suggest that in the context of activated T cells, a direct interaction between APCs and T cells during the establishment of infection could maintain latency in T cells by reducing the frequency of spontaneous virus expression.

## DISCUSSION

It is now well established that the major barrier to HIV cure is the pool of replication-competent virus that persists in latently infected cells (9). In this study, we compared HIV latency that was established through two different pathways: preactivation and postactivation. In both models, we added entry and integrase inhibitors to block spreading infection and generate a synchronous culture, including only cells that had been infected at least 3 to 5 days before sorting. This strategy was adopted to mimic a single round of replication. It minimized the likelihood of EGFP expression in these cells from permissive recently infected cells captured immediately before the onset of viral antigen expression.

The preactivation model of infection of resting T cells with CCL19 used in this study was slightly modified from the one described in our previous publications (11, 30). We showed previously that CCL19-enhanced entry into resting cells can vary across donors and is highly dependent on the multiplicity of infection (MOI) of the infecting virus (36). The present study differed from our previous studies, as here we used an EGFP-expressing virus, normalized by the 50% tissue culture infective dose (TCID<sub>50</sub>) in a limiting-dilution assay, rather than wild-type virus normalized by the reverse transcriptase (RT) activity of the transfection stock. We also used higher concentrations of CCL19 (100 nM) and IL-2 (10 U/ml). It is well known that virus at high titers can enhance HIV entry into resting CD4<sup>+</sup> T cells by chemokine receptor stimulation (37–40). The polarization of lymphocytes after the addition of virus is consistent with chemokine receptor signaling by the infecting virus, and we therefore assume that a higher inoculum of virus added to resting cells could attenuate the requirements for signaling by an exogenous chemokine (41).

We have shown markedly higher frequencies of productive infection and spontaneous virus expression in postactivation latency than in the model of preactivation latency that we used here. The responses of latent infection to LRAs, mitogens, and monocytes–anti-CD3 differed between the two models, and some of these observations could be attributed to the differences in how latency was established and the levels of proliferation of latently infected T cells receiving activation signals.

We showed previously that the underlying mechanism by which latency is maintained in preactivation latency is due to the block in virus expression postintegration (21, 41). The mechanism for maintaining latency during postactivation latency is less clear. However, the critical observation in this study was the detection of much higher frequencies of productive and spontaneous EGFP expression in the postactivation model than in the preactivation model. The correlation between productive infection and spontaneous expression (EGFP expression from unstimulated sorted EGFP<sup>−</sup> cells)

suggests that spontaneous expression from latency may represent similar mechanisms controlling virus expression before and after the sorting of latently infected T cells.

Previous studies of gene expression in individual cells have shown that both allelic expression (42) and transcriptional bursting (43, 44) are mechanisms that control gene expression in mammalian cells. The control of gene transcription in latent human T cell leukemia virus type 1 (HTLV-1) infection has shown that retroviral gene expression occurs by a process of burst expression (45). For clonally expanded cells infected with HTLV-1, latency is determined by a balance between the burst expression of Tax and the low-level, persistent expression of HTLV-1 basic leucine zipper factor (HBZ) (45). During reactivation of latent HIV infection, levels of HIV expression depend on both the frequency of bursting and the burst size (46–48). The burst size and frequency are in turn determined by the availability of transcriptional factors (48, 49), which may differ in pre- and postactivation latency models. Compared to resting CD4<sup>+</sup> T cells, activated T cells are subject to bimodal fluctuations of gene expression, dynamic and continuous changes in the gene's promoter from activated as "on" to a repressed gene as "off" (50). This would allow the positive HIV Tat feedback loop to initiate virus expression (51) more frequently in the postactivation model, resulting in more-frequent productive and spontaneous expression than that during preactivation latency. Therefore, expression from latency might be more frequently associated with a transcriptional burst in the postactivation model than in the preactivation latency model.

In the analysis of the two different latency models, we used a panel of stimuli to activate latent HIV. This included TCR stimulation to activate virus expression from latently infected cells. *In vivo*, the TCR on CD4<sup>+</sup> T cells binds to the major histocompatibility complex (MHC) expressed on APCs. In our *in vitro* analysis, we found clear differences between the two latency models in relation to the effects of interactions with an APC. The interaction of latently infected cells with both monocytes and C1R cells reduced the transcriptional burst in the postactivation latency model. The APC-T cell interaction depended on both cell-to-cell contact and functional APCs, as the inhibitory effect of monocytes was lost with irradiation. The induction of virus expression from latency during interactions with antigen-presenting cells, like monocytes, requires membrane-proximal steps (52), which suggests a contact-dependent inhibition of virus expression following coculture of latently infected cells with monocytes in postactivation latency.

The correlation between cellular proliferation and virus expression was evident in the preactivation model. In contrast, in the postactivation model, high levels of T cell proliferation were associated with low levels of virus expression, particularly following TCR signaling in the presence of monocytes. This was seen at the single-cell level by flow cytometry and could be partially but not completely explained by an expansion of uninfected cells. Although it is critical to determine the frequency of noninduced latently infected cells among proliferating T cells, the specificity of the effect on monocyte-containing cultures suggests that APC-derived interactions could maintain latency by suppressing EGFP expression in postactivation latency despite activation and proliferation. This observation is in agreement with data from our previous work (35). Coculture of myeloid cells with T cells at the time of infection maintained latency in nonproliferating T cells in a model of postactivation latency (35). Our study suggests that there is ongoing expression from latently infected cells in both pre- and postactivation latency albeit with different frequencies. We have modeled these observations in Fig. 8.

In our previous study, using transcriptome sequencing (RNA-seq) analysis of APC-T cell cocultures, we identified 4 surface proteins, including members of the sialic acid binding immunoglobulin-type lectin (SIGLEC) family, the C-type lectin domain-containing (CLEC) family, the leukocyte-associated immunoglobulin-like receptor (LILRA) family, and the G-protein-coupled receptor (GPCR) family (35). Molecules from the SIGLEC family are able to inhibit T cell activation (53). In addition, transcriptome analyses of the genes in macrophages (54, 55), monocytes (54, 55), and C1R cells (56–58) have shown the upregulation of calcium binding protein genes, including

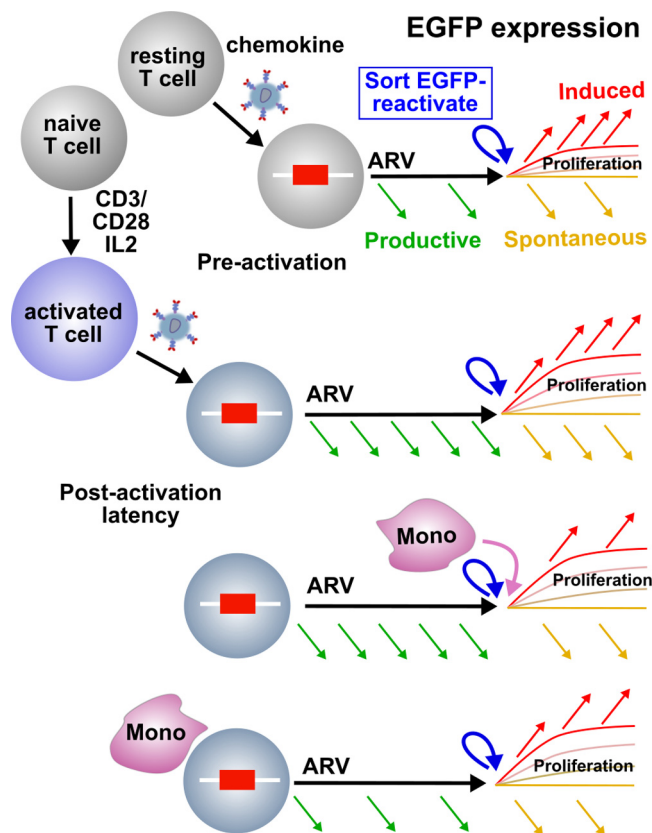


**FIG 8** Model of inducible and spontaneous EGFP expression in pre- and postactivation latency. Resting CD4<sup>+</sup> T cells were directly infected with an EGFP reporter virus, or naive T cells from the same donors were infected after TCR stimulation and the generation of memory T cells. Infected T cells were maintained with antiretrovirals from day 2 postinfection. EGFP-expressing cells were quantitated as productive infection at days 5 to 7 postinfection, and sorted EGFP<sup>-</sup> cells were recultured with and without an activating stimulus. In preactivation latency, there were low levels of productive and spontaneous expression and high levels of induced expression. High frequencies of productive and spontaneous EGFP expression were found in postactivation latency, while spontaneous and induced expression levels were similar. Monocytes inhibited EGFP expression when present during the activation of sorted EGFP<sup>-</sup> cells but also reduced spontaneous and induced expression when cultured during the initial establishment of latency.

fibrillin 2 (FBN2), desmocollin 2 (DSC2), thrombospondin 1 (THBS1), nuclear factor erythroid 2 (NFE2), stabilin 1 (STAB1), versican (VCAN), and calmodulin binding neurogranin (NRGN), which, apart from mediating cell-to-cell contact, are able to facilitate extracellular calcium binding and increase calcium-dependent physiological responses, including proliferation in resting CD4<sup>+</sup> T cells. APC-T cell interactions may activate a negative-feedback loop of the calcium-calcineurin pathway, resulting in the reduction of activation signals in activated T cells (59) and contributing to the reduction of virus expression from latency during postactivation latency.

Our observation of reduced HIV expression when some latently infected T cells interact with monocytes suggests that disrupting the interaction between APC and T cells could be targeted to reverse latency. In this study, we did not further define these interactions, but the more profound negative effect of APCs seen in postactivation latency suggests that immune checkpoints may be involved, as we have recently shown by blocking PD-1 *in vivo* and *in vitro* (60; V. A. Evans, unpublished data).

There are some limitations to this study. We used an EGFP reporter virus to define productive infection following initial infection and to measure spontaneous and activation-induced virus expression from latency. Although the EGFP reporter virus provides a useful tool to study virus expression, measurement of EGFP expression using FCM represents intracellular viral protein expression but does not directly measure virus

**TABLE 1** Summary of differences found in responses to reactivation between *in vitro* latency models

Observation	Response in <i>in vitro</i> latency model	
	Preactivation	Postactivation
Spontaneous virus expression	Low	High
Response to monocyte–anti-CD3 stimulation	High	Low
Response to LRAs	Moderate	Low
Proliferative response to activation	Moderate	High
Correlation between proliferation and expression	Yes	No
Induced expression in nonproliferating cells	Low	High
Induced expression in proliferating cells	Moderate	Low

production and the completion of the virus life cycle. However, we previously showed a correlation between EGFP expression and virus production (21) in the preactivation model.

In addition, we detected different frequencies of spontaneous EGFP expression from latently infected cells in the two *in vitro* latency models. A potential explanation for this observation is that by using EGFP expression as the readout of latency or productive infection *in vitro*, we may be including cells that may express viral mRNA but not detectable viral protein/EGFP. The sorted EGFP<sup>−</sup> cells may contain mixed populations of RNA<sup>+</sup> EGFP<sup>−</sup> and RNA<sup>−</sup> EGFP<sup>−</sup> cells. The likelihood of RNA<sup>+</sup> EGFP<sup>−</sup> cells proceeding to spontaneous EGFP expression may be high. We have tried to minimize this potential confounder by adding antiretrovirals to the cultures shortly after infection, but the use of a dual-reporter virus for measuring the frequency of latent and inducible proviruses would help define these populations more clearly. For the viruses in the present study, however, the expression of the marker for latency is variable (61). Alternatively, screening of the EGFP-negative population for RNA expression using single-cell hybridization, which has been developed recently, to remove RNA<sup>+</sup> EGFP<sup>−</sup> cells (62) would enable enrichment for the EGFP<sup>−</sup> latent population *in vitro*.

In conclusion, we have shown differences in responses to stimulation when monocytes are included in cocultures during pre- and postactivation latency (Table 1). The presence of APCs in the cocultures during the establishment of latency or during latency reversal was able to control virus expression independent of induced proliferation. This suggests that signaling beyond the TCR and CD28 are important for maintaining latent infection.

The observed differences between pre- and postactivation latency and the different responses to latency reversal suggest that the pathway by which latency is established may determine optimal signals for the reactivation and subsequent clearance of latently infected cells. The activation status of the T cells at the time of infection may be independent of the ability to establish latent infection, but the maintenance of latency will depend on factors that drive or inhibit latency reversal. The stochastic process of spontaneous activation in postactivation latency may drive the persistence of latency and the final repertoire of cells that constitute the latent reservoir.

## MATERIALS AND METHODS

**Cell isolation and culture.** RPMI 1640 medium (Invitrogen, Carlsbad, CA) was supplemented with 2 mM L-glutamine, 100 U/ml penicillin, and 0.1 μg/ml of streptomycin plus 10% heat-inactivated fetal calf serum (FCS) (Lonza, Collingwood, Australia) to make RF10 or 10% heat-inactivated human serum to make RH10.

Peripheral blood mononuclear cells (PBMCs) were isolated by Ficoll-Paque density gradient centrifugation (GE Healthcare, Chalfont St. Giles, UK) from buffy coats obtained from the Australian Red Cross Blood Service (Southbank, Melbourne, Australia). Resting CD4<sup>+</sup> T cells were negatively selected by magnetically activated cell sorting (MACS) using goat anti-mouse IgG beads (Miltenyi Biotec, Cologne, Germany) and the AutoMACS Pro system (Miltenyi Biotec), using a cocktail of antibodies to CD8, CD19, CD11b, CD14, CD16, HLA-DR, and CD69, as previously described (11, 30). The purity of the isolated rCD4<sup>+</sup> T cells was always ≥95%, as assessed by FCM.

Naive T cells were negatively selected from resting CD4<sup>+</sup> T cells using CD45RO beads and magnetically activated cell sorting. Allogeneic monocytes were positively selected by using CD14 antibody (FMC17 hybridoma supernatant, provided by Heddy Zola, Flinders Medical Centre) and goat anti-mouse



IgG beads (Miltenyi Biotec) on a MACS cell sorter. MDMs were differentiated from monocytes following culture in human-serum-containing medium (RH10) for 8 days.

The EBV-transformed B cell line C1R (provided by Lyudmila Kostenko, McCluskey Lab, The Peter Doherty Institute) was cultured in RF10.

**Preparation of HIV and infection.** The Nef-competent HIV<sub>NL4.3</sub> construct with EGFP inserted at positions 8787 to 9506 between the Env and Nef regions (pNL4.3-EGFP) was kindly provided by Yasuko Tsunetsugu-Yokota (National Institute of Infectious Diseases, Tokyo, Japan) (63). The virus stock was generated by using FuGene (Promega, Madison, WI) transfection into 293T cells, as previously described (16, 30). The MOI was determined by an endpoint dilution assay in PHA-activated PBMCs, and the TCID<sub>50</sub> was calculated as described previously (64).

**In vitro latency assays.** To establish preactivation latency, rCD4<sup>+</sup> T cells were isolated and cultured in medium alone or with the chemokine CCL19 at a final concentration of 100 nM (R&D, Minneapolis, MN) for 24 h prior to infection (11, 30, 36). Cells were infected with NL4.3-EGFP at an MOI of 0.5 and cultured with IL-2 (10 U/ml). The postactivation model was adapted from a method reported previously (14, 65), in which  $5 \times 10^5$  naive T cells were isolated from rCD4<sup>+</sup> T cells of healthy PBMCs and activated with anti-CD3/anti-CD28 beads at a ratio of 1:1, according to the manufacturer's protocol (Dyna/Invitrogen). Nonpolarized CD4<sup>+</sup> memory T cells were generated by the addition of anti-IL-4 (1  $\mu$ g/ml; BD Biosciences, San Jose, CA), anti-IL-12 (2  $\mu$ g/ml; BD Biosciences), and recombinant human transforming growth factor  $\beta$  (TGF- $\beta$ ) (10 ng/ml; R&D). The medium was further supplemented with 10% human serum and 200 U/ml IL-2 (Roche, Mannheim, Germany). After 3 days, beads were removed by using DynaMag-Spin (Dyna/Invitrogen), and cells were cultured at a concentration of  $1 \times 10^6$  cells/ml of medium containing IL-2 (30 U/ml). Cells were infected with the same virus stock at the same MOI. In both pre- and postactivation latency, the antiretroviral integrase inhibitor raltegravir (Ral) (1  $\mu$ M) and the fusion inhibitor T20 (0.1  $\mu$ g/ml; AIDS Reagent Program, National Institutes of Health, Germantown, MD) were added to each culture at 48 h postinfection to block further rounds of infection.

At day 5 postinfection in the preactivation model and at day 7 in the postactivation model, cells expressing EGFP (designated productive infection) and EGFP-negative cells (designated latent infection) were quantitated, and the EGFP<sup>-</sup> cells were sorted by using FCM (MoFloAstrios; Beckman Coulter, Brea, CA). The EGFP<sup>-</sup> cells (latent infection) were recultured without stimulation to detect background or spontaneous expression or with different activation stimuli to detect activation-induced EGFP expression (induced expression) (Fig. 1).

The sorted non-EGFP-expressing cells were cocultured in medium supplemented with antivirals only or stimulated on plates coated with anti-CD3 (20  $\mu$ g/ml of anti-human CD3 $\epsilon$ , clone UCHT1; BD Biosciences), soluble anti-CD28 (3.6  $\mu$ g/ml, clone L293; BD Biosciences), or anti-CD3/anti-CD28 beads (1:1 ratio; Dynal/Invitrogen) and mitogens, including PMA (50 ng/ml; Sigma-Aldrich, St. Louis, MO) combined with ionomycin (500 ng/ml) or PHA (10  $\mu$ g/ml; Thermo Fisher Scientific, Waltham, MA), Pan (30 nM; Selleck Chemicals, Houston, TX), Rom (40 nM; Selleck Chemicals), JQ1 (1  $\mu$ M; Sigma-Aldrich), CTN (10 nM; Sigma-Aldrich), IL-7 (50 ng/ml; Sigma-Aldrich), or Bryo-1 (10 nM; Selleck). The frequencies of EGFP expression from unstimulated or DMSO control cultures were used as a measure of background or spontaneous expression.

Monocytes were used with T cells at 1:10 ratios either alone or with soluble anti-CD3 (20  $\mu$ g/ml; BD Biosciences). For some experiments, allogeneic monocytes were irradiated with cobalt 60 (<sup>60</sup>Co) at 3,000 rads before coculturing with latent cells.

All the reactivation experiments were performed in the presence of raltegravir and T20. After 72 h, the EGFP expression level was quantified by FCM and compared to that in unstimulated cultures. Monocytes were excluded from the analysis by using phycoerythrin (PE)-conjugated anti-CD14 (BD Biosciences).

**Coculture of HIV-infected T cells with APCs.** To reduce spontaneous virus expression in the postactivation latency model, HIV-infected CD4<sup>+</sup> T cells were cocultured with syngeneic monocytes, syngeneic MDMs, and the irradiated EBV-transformed B cell line C1R. APCs were added to the cultures at 48 h postinfection with infected T cells at 1:10 ratios. The level of spontaneous EGFP expression in unstimulated cultures was measured. In some experiments, as indicated, direct interactions between APCs and infected T cells were blocked by culture in a transwell (0.4- $\mu$ m Costar plates; Corning, NY).

**Measurement of HIV infection and reactivation by flow cytometry.** Infection in the cell cultures was monitored by EGFP expression using FCM performed on a FACSCalibur (BD Biosciences) or an LSRII (BD Biosciences) instrument. Cell sorting of HIV-infected cells was performed by using an Astrios cell sorter (Beckman Coulter, CA). CellQuest version 3.0 (BD Biosciences), FACSDiva version 8.0.2 (BD Biosciences), or Summit version 6.3 (Beckman Coulter) was used for acquisition, and Weasel software version 3.3 was used for analysis. Routinely, 50,000 to 100,000 events were collected per sample. Live gating was based on forward-versus-side-scatter plots, and in some experiments, cell viability was determined by using the eFluor780 fixable viability dye (Affymetrix-eBioscience, San Diego, CA). EGFP expression was reported as the number of EGFP-positive cells per 10,000 live cells.

**Measurement of cell proliferation.** The sorted EGFP<sup>-</sup> cells were stained with eFluor670 proliferation dye (Affymetrix-eBioscience) prior to coculture, according to the manufacturer's protocol. Briefly, EGFP<sup>-</sup> cells were washed and resuspended in medium containing proliferation dye at a final concentration of 5  $\mu$ M. Cells were incubated at 37°C for 10 min. After incubation, cells were washed with cold RPMI (10% FCS) and cultured. The levels of proliferation in each culture were measured at 72 h postactivation by FCM. Proliferation was quantitated by using Weasel cell cycle analysis (v3.3) and compared to that in unstimulated cultures.

**Quantitative PCR assays for HIV.** The HIV DNA level was quantified as described previously (66). Briefly, a total of  $5 \times 10^5$  to  $1 \times 10^6$  EGFP<sup>+</sup> cells were sorted and cultured with antiretrovirals alone or cocultured with allogeneic monocytes, allogeneic monocytes and soluble anti-CD3 (20  $\mu$ g/ml), or anti-CD3/anti-CD28 beads (1:1 ratio). At 72 h postactivation, cells were collected, washed, and pelleted at  $16,000 \times g$  for 5 min. Cell pellets were resuspended in lysis buffer (0.1 M Tris HCl [pH 8], 0.5 M KCl, 10 mg/ml proteinase K, double-distilled water [ddH<sub>2</sub>O]) (67, 68) and digested for 1 h by using a thermal cycler (Bio-Rad, Hercules, CA) following incubation at 56°C for 60 min and at 95°C for 10 min. Total HIV DNA was amplified in 50  $\mu$ l of the reaction mix. Data were collected with the Stratagene MX3005 pro real-time PCR system (Agilent Technologies). Primers specific for the human CCR5 genes were used to quantify the number of cells per reaction. The copy number of HIV DNA was quantified by using a 10-fold serial dilution of a chronically infected HIV cell line, ACH2, ranging from  $2 \times 10^0$  to  $2 \times 10^4$  copies of HIV DNA and reported per million CCR5 cells.

**Statistical analysis.** The Wilcoxon matched-pairs signed-rank test was used for all the paired analyses between samples, and the Mann-Whitney test was used for nonpaired analysis, when the number of data points was more than 6. When the numbers of data points were 6 or fewer, we used Student's paired or unpaired *t* test. Spearman's test was used to determine correlations. Statistical analysis was performed by using Graph Pad Prism v 6.0 (GraphPad Software, La Jolla, CA) or R (version 3.3.2) (69).

## SUPPLEMENTAL MATERIAL

Supplemental material for this article may be found at <https://doi.org/10.1128/JVI.02225-17>.

**SUPPLEMENTAL FILE 1**, PDF file, 2.5 MB.

## ACKNOWLEDGMENTS

We thank all the blood donors recruited by the Australian Red Cross Blood Transfusion Service as normal blood donors for the use of their blood products for research, Ashish Nadir (The Peter Doherty Institute for Infection and Immunity, Australia) for his technical assistance, all the staff at the ImmunoID flow cytometry facility (The Peter Doherty Institute for Infection and Immunity, Australia) for their assistance with cell sorting, and Paul Gorry and his team (The RMIT University, Bundoora, Melbourne, Australia) for providing human serum. Renee Van der Sluis provided technical advice and intellectual input.

This work was supported by NHMRC project grant APP1058891. S.R.L. and P.U.C. are supported by the Division of AIDS, National Institute of Allergy and Infectious Diseases, U.S. National Institutes of Health (Delaney AIDS Research Enterprise [DARE]; U19AI096109). S.R.L. was supported by a NHMRC practitioner fellowship. S.D.R. was the recipient of an Australian postgraduate award.

P.U.C., S.R.L., and S.D.R. designed the study. S.D.R. carried out cell isolation, infection, sorting, and reactivation experiments. S.D.R. performed the FCM analysis of the data with the help of P.U.C. J.J.C., and H.K.L., and A.R. assisted with the setup of the experiment. S.D.R. and P.U.C. analyzed the data. S.D.R. and P.U.C. performed statistical analysis. S.D.R., S.R.L., and P.U.C. wrote the manuscript.

## REFERENCES

- Chun TW, Stuyver L, Mizell SB, Ehler LA, Mican JA, Baseler M, Lloyd AL, Nowak MA, Fauci AS. 1997. Presence of an inducible HIV-1 latent reservoir during highly active antiretroviral therapy. *Proc Natl Acad Sci U S A* 94:13193–13197.
- Finzi D, Hermankova M, Pierson T, Carruth LM, Buck C, Chaisson RE, Quinn TC, Chadwick K, Margolick J, Brookmeyer R, Gallant J, Markowitz M, Ho DD, Richman DD, Siliciano RF. 1997. Identification of a reservoir for HIV-1 in patients on highly active antiretroviral therapy. *Science* 278:1295–1300. <https://doi.org/10.1126/science.278.5341.1295>.
- Shan L, Deng K, Gao H, Xing S, Capoferri AA, Durand CM, Rabi SA, Laird GM, Kim M, Hosmane NN. 2017. Transcriptional reprogramming during effector-to-memory transition renders CD4<sup>+</sup> T cells permissive for latent HIV-1 infection. *Immunity* 47:766–775. <https://doi.org/10.1016/j.immuni.2017.09.014>.
- Buzon MJ, Sun H, Li C, Shaw A, Seiss K, Ouyang Z, Martin-Gayo E, Leng J, Henrich TJ, Li JZ, Pereyra F, Zurakowski R, Walker BD, Rosenberg ES, Yu XG, Lichterfeld M. 2014. HIV-1 persistence in CD4<sup>+</sup> T cells with stem cell-like properties. *Nat Med* 20:139–142. <https://doi.org/10.1038/nm.3445>.
- Chomont N, El-Far M, Ancuta P, Trautmann L, Procopio FA, Yassine-Diab B, Boucher G, Boulassel M-R, Ghattas G, Brenchley JM, Schacker TW, Hill BJ, Douek DC, Routy J-P, Haddad EK, Sekaly R-P. 2009. HIV reservoir size and persistence are driven by T cell survival and homeostatic proliferation. *Nat Med* 15:893–900. <https://doi.org/10.1038/nm.1972>.
- Pallikkuth S, Sharkey M, Babic DZ, Gupta S, Stone GW, Fischl MA, Stevenson M, Pahwa S. 2016. Peripheral T follicular helper cells are the major HIV reservoir within central memory CD4 T cells in peripheral blood from chronically HIV-infected individuals on combination antiretroviral therapy. *J Virol* 90:2718–2728. <https://doi.org/10.1128/JVI.02883-15>.
- Lee GQ, Orlova-Fink N, Einkauf K, Chowdhury FZ, Sun X, Harrington S, Kuo H-H, Hua S, Chen H-R, Ouyang Z. 2017. Clonal expansion of genome-intact HIV-1 in functionally polarized Th1 CD4<sup>+</sup> T cells. *J Clin Invest* 127:2689–2696. <https://doi.org/10.1172/JCI93289>.
- Bui JK, Sobolewski MD, Keele BF, Spindler J, Musick A, Wiegand A, Luke BT, Shao W, Hughes SH, Coffin JM. 2017. Proviruses with identical sequences comprise a large fraction of the replication-

- competent HIV reservoir. *PLoS Pathog* 13:e1006283. <https://doi.org/10.1371/journal.ppat.1006283>.
9. Ho YC, Shan L, Hosmane NN, Wang J, Laskey SB, Rosenbloom DI, Lai J, Blankson JN, Siliciano JD, Siliciano RF. 2013. Replication-competent non-induced proviruses in the latent reservoir increase barrier to HIV-1 cure. *Cell* 155:540–551. <https://doi.org/10.1016/j.cell.2013.09.020>.
  10. Simonetti FR, Sobolewski MD, Fyne E, Shao W, Spindler J, Hattori J, Anderson EM, Watters SA, Hill S, Wu X. 2016. Clonally expanded CD4<sup>+</sup> T cells can produce infectious HIV-1 in vivo. *Proc Natl Acad Sci U S A* 113:1883–1888. <https://doi.org/10.1073/pnas.1522675113>.
  11. Saleh S, Solomon A, Wightman F, Xhilaga M, Cameron PU, Lewin SR. 2007. CCR7 ligands CCL19 and CCL21 increase permissiveness of resting memory CD4<sup>+</sup> T cells to HIV-1 infection: a novel model of HIV-1 latency. *Blood* 110:4161–4164. <https://doi.org/10.1182/blood-2007-06-097907>.
  12. Swiggard WJ, Baytop C, Yu JJ, Dai J, Li C, Schretzenmair R, Theodosopoulos T, O'Doherty U. 2005. Human immunodeficiency virus type 1 can establish latent infection in resting CD4<sup>+</sup> T cells in the absence of activating stimuli. *J Virol* 79:14179–14188. <https://doi.org/10.1128/JVI.79.22.14179-14188.2005>.
  13. Lassen KG, Hebbeler AM, Bhattacharyya D, Lobritz MA, Greene WC. 2012. A flexible model of HIV-1 latency permitting evaluation of many primary CD4 T-cell reservoirs. *PLoS One* 7:e30176. <https://doi.org/10.1371/journal.pone.0030176>.
  14. Bosque A, Planelles V. 2009. Induction of HIV-1 latency and reactivation in primary memory CD4<sup>+</sup> T cells. *Blood* 113:58–65. <https://doi.org/10.1182/blood-2008-07-168393>.
  15. Marini A, Harper JM, Romero F. 2008. An in vitro system to model the establishment and reactivation of HIV-1 latency. *J Immunol* 181:7713–7720. <https://doi.org/10.4049/jimmunol.181.11.7713>.
  16. Evans VA, Kumar N, Filali A, Procopio FA, Yegorov O, Goulet JP, Saleh S, Haddad EK, da Fonseca Pereira C, Ellenberg PC. 2013. Myeloid dendritic cells induce HIV-1 latency in non-proliferating CD4<sup>+</sup> T cells. *PLoS Pathog* 9:e1003799. <https://doi.org/10.1371/journal.ppat.1003799>.
  17. Cillo AR, Sobolewski MD, Bosch RJ, Fyne E, Piatak M, Jr, Coffin JM, Mellors JW. 2014. Quantification of HIV-1 latency reversal in resting CD4<sup>+</sup> T cells from patients on suppressive antiretroviral therapy. *Proc Natl Acad Sci U S A* 111:7078–7083. <https://doi.org/10.1073/pnas.1402873111>.
  18. Hosmane NN, Kwon KJ, Bruner KM, Capoferri AA, Beg S, Rosenbloom DI, Keele BF, Ho Y-C, Siliciano JD, Siliciano RF. 2017. Proliferation of latently infected CD4<sup>+</sup> T cells carrying replication-competent HIV-1: potential role in latent reservoir dynamics. *J Exp Med* 214:959–972. <https://doi.org/10.1084/jem.20170193>.
  19. Bullen CK, Laird GM, Durand CM, Siliciano JD, Siliciano RF. 2014. New ex vivo approaches distinguish effective and ineffective single agents for reversing HIV-1 latency in vivo. *Nat Med* 20:425–429. <https://doi.org/10.1038/nm.3489>.
  20. Spina CA, Anderson J, Archin NM, Bosque A, Chan J, Famiglietti M, Greene WC, Kashuba A, Lewin SR, Margolis DM. 2013. An in-depth comparison of latent HIV-1 reactivation in multiple cell model systems and resting CD4<sup>+</sup> T cells from aviremic patients. *PLoS Pathog* 9:e1003834. <https://doi.org/10.1371/journal.ppat.1003834>.
  21. Saleh S, Wightman F, Ramanayake S, Alexander M, Kumar N, Khoury G, Pereira C, Purcell D, Cameron PU, Lewin SR. 2011. Expression and reactivation of HIV in a chemokine induced model of HIV latency in primary resting CD4<sup>+</sup> T cells. *Retrovirology* 8:80. <https://doi.org/10.1186/1742-4690-8-80>.
  22. Novis CL, Archin NM, Buzon MJ, Verdin E, Round JL, Lichtenfeld M, Margolis DM, Planelles V, Bosque A. 2013. Reactivation of latent HIV-1 in central memory CD4<sup>+</sup> T cells through TLR-1/2 stimulation. *Retrovirology* 10:119. <https://doi.org/10.1186/1742-4690-10-119>.
  23. Spivak AM, Larragoite ET, Coletti ML, Macedo AB, Martins LJ, Bosque A, Planelles V. 2016. Janus kinase inhibition suppresses PKC-induced cytokine release without affecting HIV-1 latency reversal ex vivo. *Retrovirology* 13:88. <https://doi.org/10.1186/s12977-016-0319-0>.
  24. Tsai P, Wu G, Baker CE, Thayer WO, Spagnuolo RA, Sanchez R, Barrett S, Howell B, Margolis D, Hazuda DJ, Archin NM, Garcia JV. 2016. In vivo analysis of the effect of panobinostat on cell-associated HIV RNA and DNA levels and latent HIV infection. *Retrovirology* 13:36. <https://doi.org/10.1186/s12977-016-0268-7>.
  25. van der Sluis RM, van Montfort T, Pollakis G, Sanders RW, Speijer D, Berkhout B, Jeeninga RE. 2013. Dendritic cell-induced activation of latent HIV-1 provirus in actively proliferating primary T lymphocytes. *PLoS Pathog* 9:e1003259. <https://doi.org/10.1371/journal.ppat.1003259>.
  26. van der Sluis RM, van Capel TM, Speijer D, Sanders RW, Berkhout B, de Jong EC, Jeeninga RE, van Montfort T. 2015. Dendritic cell type-specific HIV-1 activation in effector T cells: implications for latent HIV-1 reservoir establishment. *AIDS* 29:1003–1014. <https://doi.org/10.1097/QAD.0000000000000637>.
  27. Walker C, Betters F, Pichler WJ. 1987. Activation of T cells by cross-linking an anti-CD3 antibody with a second anti-T cell antibody: mechanism and subset-specific activation. *Eur J Immunol* 17:873–880. <https://doi.org/10.1002/eji.1830170622>.
  28. Gunn MD, Tangemann K, Tam C, Cyster JG, Rosen SD, Williams LT. 1998. A chemokine expressed in lymphoid high endothelial venules promotes the adhesion and chemotaxis of naive T lymphocytes. *Proc Natl Acad Sci U S A* 95:258–263.
  29. Ziegler E, Oberbarnscheidt M, Bulfone-Paus S, Förster R, Kunzendorf U, Krautwald S. 2007. CCR7 signaling inhibits T cell proliferation. *J Immunol* 179:6485–6493. <https://doi.org/10.4049/jimmunol.179.10.6485>.
  30. Cameron PU, Saleh S, Sallmann G, Solomon A, Wightman F, Evans VA, Boucher G, Haddad EK, Sekaly RP, Harman AN, Anderson JL, Jones KL, Mak J, Cunningham AL, Jaworowski A, Lewin SR. 2010. Establishment of HIV-1 latency in resting CD4<sup>+</sup> T cells depends on chemokine-induced changes in the actin cytoskeleton. *Proc Natl Acad Sci U S A* 107:16934–16939. <https://doi.org/10.1073/pnas.1002894107>.
  31. Chun T-W, Justement JS, Lempicki RA, Yang J, Dennis G, Hallahan CW, Sanford C, Pandya P, Liu S, McLaughlin M. 2003. Gene expression and viral production in latently infected, resting CD4<sup>+</sup> T cells in viremic versus aviremic HIV-infected individuals. *Proc Natl Acad Sci U S A* 100:1908–1913. <https://doi.org/10.1073/pnas.0437640100>.
  32. Elliott JH, Wightman F, Solomon A, Gneim K, Ahlers J, Cameron MJ, Smith MZ, Spelman T, McMahon J, Velayudham P. 2014. Activation of HIV transcription with short-course vorinostat in HIV-infected patients on suppressive antiretroviral therapy. *PLoS Pathog* 10:e1004473. <https://doi.org/10.1371/journal.ppat.1004473>.
  33. Lewin S, Vesanen M, Kostrikis L, Hurley A, Duran M, Zhang L, Ho D, Markowitz M. 1999. Use of real-time PCR and molecular beacons to detect virus replication in human immunodeficiency virus type 1-infected individuals on prolonged effective antiretroviral therapy. *J Virol* 73:6099–6103.
  34. Pace MJ, Graf EH, Agosto LM, Mexas AM, Male F, Brady T, Bushman FD, O'Doherty U. 2012. Directly infected resting CD4<sup>+</sup> T cells can produce HIV Gag without spreading infection in a model of HIV latency. *PLoS Pathog* 8:e1002818. <https://doi.org/10.1371/journal.ppat.1002818>.
  35. Kumar NA, Cheong K, Powell DR, da Fonseca Pereira C, Anderson J, Evans VA, Lewin SR, Cameron PU. 2015. The role of antigen presenting cells in the induction of HIV-1 latency in resting CD4<sup>+</sup> T-cells. *Retrovirology* 12:76. <https://doi.org/10.1186/s12977-015-0204-2>.
  36. Anderson JL, Mota TM, Evans VA, Kumar N, Rezaei SD, Cheong K, Solomon A, Wightman F, Cameron PU, Lewin SR. 2016. Understanding factors that modulate the establishment of HIV latency in resting CD4<sup>+</sup> T-cells in vitro. *PLoS One* 11:e0158778. <https://doi.org/10.1371/journal.pone.0158778>.
  37. Yoder A, Yu D, Dong L, Iyer SR, Xu X, Kelly J, Liu J, Wang W, Vorster PJ, Agulto L. 2008. HIV envelope-CXCR4 signaling activates cofilin to overcome cortical actin restriction in resting CD4 T cells. *Cell* 134:782–792. <https://doi.org/10.1016/j.cell.2008.06.036>.
  38. Lin Y-L, Mettling C, Portalès P, Réant B, Robert-Hebmann V, Reynes J, Clot J, Corbeau P. 2006. The efficiency of R5 HIV-1 infection is determined by CD4 T-cell surface CCR5 density through Gαi-protein signaling. *AIDS* 20:1369–1377. <https://doi.org/10.1097/01.aids.0000233570.51899.e2>.
  39. Weissman D, Rabin RL, Arthos J, Rubbert A, Dybul M, Swofford R, Venkatesan S, Farber JM, Fauci AS. 1997. Macrophage-tropic HIV and SIV envelope proteins induce a signal through the CCR5 chemokine receptor. *Nature* 389:981–985. <https://doi.org/10.1038/40173>.
  40. Pace MJ, Agosto L, O'Doherty U. 2011. R5 HIV env and vesicular stomatitis virus G protein cooperate to mediate fusion to naive CD4<sup>+</sup> T cells. *J Virol* 85:644–648. <https://doi.org/10.1128/JVI.01851-10>.
  41. Saleh S, Lu HK, Evans V, Harisson D, Zhou J, Jaworowski A, Sallmann G, Cheong KY, Mota TM, Tennakoon S, Angelovich TA, Anderson J, Harman A, Cunningham A, Gray L, Churchill M, Mak J, Drummer H, Vatakis DN, Lewin SR, Cameron PU. 2016. HIV integration and the establishment of latency in CCL19-treated resting CD4<sup>+</sup> T cells require activation of NF-κB. *Retrovirology* 13:49. <https://doi.org/10.1186/s12977-016-0284-7>.
  42. Deng Q, Ramsköld D, Reinius B, Sandberg R. 2014. Single-cell RNA-seq reveals dynamic, random monoallelic gene expression in mammalian cells. *Science* 343:193–196. <https://doi.org/10.1126/science.1245316>.

43. Raj A, Peskin CS, Tranchina D, Vargas DY, Tyagi S. 2006. Stochastic mRNA synthesis in mammalian cells. *PLoS Biol* 4:e309. <https://doi.org/10.1371/journal.pbio.0040309>.
44. Suter DM, Molina N, Gatfield D, Schneider K, Schibler U, Naef F. 2011. Mammalian genes are transcribed with widely different bursting kinetics. *Science* 332:472–474. <https://doi.org/10.1126/science.1198817>.
45. Macchi B, Balestrieri E, Frezza C, Grelli S, Valletta E, Marçais A, Marino-Merlo F, Turpin J, Bangham CR, Hermine O. 2017. Quantification of HTLV-1 reverse transcriptase activity in ATL patients treated with zidovudine and interferon- $\alpha$ . *Blood Adv* 1:748–752. <https://doi.org/10.1182/bloodadvances.2016001370>.
46. Skupsky R, Burnett JC, Foley JE, Schaffer DV, Arkin AP. 2010. HIV promoter integration site primarily modulates transcriptional burst size rather than frequency. *PLoS Comput Biol* 6:e1000952. <https://doi.org/10.1371/journal.pcbi.1000952>.
47. Singh A, Razoooky B, Cox CD, Simpson ML, Weinberger LS. 2010. Transcriptional bursting from the HIV-1 promoter is a significant source of stochastic noise in HIV-1 gene expression. *Biophys J* 98:L32–L34. <https://doi.org/10.1016/j.bpj.2010.03.001>.
48. Dey SS, Foley JE, Limsirichai P, Schaffer DV, Arkin AP. 2015. Orthogonal control of expression mean and variance by epigenetic features at different genomic loci. *Mol Syst Biol* 11:806. <https://doi.org/10.15252/msb.20145704>.
49. Dar RD, Razoooky BS, Weinberger LS, Cox CD, Simpson ML. 2015. The low noise limit in gene expression. *PLoS One* 10:e0140969. <https://doi.org/10.1371/journal.pone.0140969>.
50. Weinberger LS, Dar RD, Simpson ML. 2008. Transient-mediated fate determination in a transcriptional circuit of HIV. *Nat Genet* 40:466–470. <https://doi.org/10.1038/ng.116>.
51. Weinberger LS, Burnett JC, Toettcher JE, Arkin AP, Schaffer DV. 2005. Stochastic gene expression in a lentiviral positive-feedback loop: HIV-1 Tat fluctuations drive phenotypic diversity. *Cell* 122:169–182. <https://doi.org/10.1016/j.cell.2005.06.006>.
52. Dustin ML, Springer TA. 1989. T-cell receptor cross-linking transiently stimulates adhesiveness through LFA-1. *Nature* 341:619–624. <https://doi.org/10.1038/341619a0>.
53. Whitney G, Wang S, Chang H, Cheng KY, Lu P, Zhou XD, Yang WP, McKinnon M, Longphre M. 2001. A new siglec family member, siglec-10, is expressed in cells of the immune system and has signaling properties similar to CD33. *Eur J Biochem* 268:6083–6096. <https://doi.org/10.1046/j.0014-2956.2001.02543.x>.
54. Maouche S, Poirier O, Godefroy T, Olaso R, Gut I, Collet J-P, Montalescot G, Cambien F. 2008. Performance comparison of two microarray platforms to assess differential gene expression in human monocyte and macrophage cells. *BMC Genomics* 9:302. <https://doi.org/10.1186/1471-2164-9-302>.
55. Liu H, Shi B, Huang C-C, Eksarko P, Pope RM. 2008. Transcriptional diversity during monocyte to macrophage differentiation. *Immunol Lett* 117:70–80. <https://doi.org/10.1016/j.imlet.2007.12.012>.
56. Çalıřkan M, Cusanovich DA, Ober C, Gilad Y. 2011. The effects of EBV transformation on gene expression levels and methylation profiles. *Hum Mol Genet* 20:1643–1652. <https://doi.org/10.1093/hmg/ddr041>.
57. Min JL, Barrett A, Watts T, Pettersson FH, Lockstone HE, Lindgren CM, Taylor JM, Allen M, Zondervan KT, McCarthy ML. 2010. Variability of gene expression profiles in human blood and lymphoblastoid cell lines. *BMC Genomics* 11:96. <https://doi.org/10.1186/1471-2164-11-96>.
58. Hertle ML, Popp C, Petermann S, Maier S, Kremmer E, Lang R, Mages J, Kempkes B. 2009. Differential gene expression patterns of EBV infected EBNA-3A positive and negative human B lymphocytes. *PLoS Pathog* 5:e1000506. <https://doi.org/10.1371/journal.ppat.1000506>.
59. Marangoni F, Murooka TT, Manzo T, Kim EY, Carrizosa E, Elpek NM, Mempel TR. 2013. The transcription factor NFAT exhibits signal memory during serial T cell interactions with antigen-presenting cells. *Immunity* 38:237–249. <https://doi.org/10.1016/j.immuni.2012.09.012>.
60. Le Garff G, Samri A, Lambert-Niclot S, Even S, Lavolé A, Cadranet J, Spano J-P, Autran B, Marcelin A-G, Guihot A. 2017. Transient HIV-specific T cells increase and inflammation in an HIV-infected patient treated with nivolumab. *AIDS* 31:1048–1051. <https://doi.org/10.1097/QAD.0000000000001429>.
61. Chavez L, Calvanese V, Verdin E. 2015. HIV latency is established directly and early in both resting and activated primary CD4 T cells. *PLoS Pathog* 11:e1004955. <https://doi.org/10.1371/journal.ppat.1004955>.
62. Baxter AE, Niessl J, Fromentin R, Richard J, Porichis F, Charlebois R, Massanella M, Brassard N, Alshafiq N, Delgado G-G. 2016. Single-cell characterization of viral translation-competent reservoirs in HIV-infected individuals. *Cell Host Microbe* 20:368–380. <https://doi.org/10.1016/j.chom.2016.07.015>.
63. Yamamoto T, Tsunetsugu-Yokota Y, Mitsuki YY, Mizukoshi F, Tsuchiya T, Terahara K, Inagaki Y, Yamamoto N, Kobayashi K, Inoue J. 2009. Selective transmission of R5 HIV-1 over X4 HIV-1 at the dendritic cell-T cell infectious synapse is determined by the T cell activation state. *PLoS Pathog* 5:e1000279. <https://doi.org/10.1371/journal.ppat.1000279>.
64. Reed LJ, Muench H. 1938. A simple method of estimating fifty per cent endpoints. *Am J Epidemiol* 27:493–497. <https://doi.org/10.1093/oxfordjournals.aje.a118408>.
65. Bosque A, Planelles V. 2011. Studies of HIV-1 latency in an ex vivo model that uses primary central memory T cells. *Methods* 53:54–61. <https://doi.org/10.1016/j.jymeth.2010.10.002>.
66. Ellery PJ, Tippett E, Chiu Y-L, Paukovics G, Cameron PU, Solomon A, Lewin SR, Gorry PR, Jaworowski A, Greene WC. 2007. The CD16<sup>+</sup> monocyte subset is more permissive to infection and preferentially harbors HIV-1 in vivo. *J Immunol* 178:6581–6589. <https://doi.org/10.4049/jimmunol.178.10.6581>.
67. Fromentin R, Bakeman W, Lawani MB, Khoury G, Hartogensis W, DaFonseca S, Killian M, Epling L, Hoh R, Sinclair E, Hecht FM, Bacchetti P, Deeks SG, Lewin SR, Sékaly R-P, Chomont N. 2016. CD4<sup>+</sup> T cells expressing PD-1, TIGIT and LAG-3 contribute to HIV persistence during ART. *PLoS Pathog* 12:e1005761. <https://doi.org/10.1371/journal.ppat.1005761>.
68. Vandergeeten C, Fromentin R, Merlini E, Lawani MB, DaFonseca S, Bakeman W, McNulty A, Ramgopal M, Michael N, Kim JH, Ananworanich J, Chomont N. 2014. Cross-clade ultrasensitive PCR-based assays to measure HIV persistence in large-cohort studies. *J Virol* 88:12385–12396. <https://doi.org/10.1128/JVI.00609-14>.
69. Ihaka R, Gentleman R. 1996. R: a language for data analysis and graphics. *J Comput Graph Stat* 5:299–314. <https://doi.org/10.1080/10618600.1996.10474713>.